ELSEVIER

Journal of Alloys and Compounds 323–324 (2001) 481–485

Journal of ALLOYS AND COMPOUNDS

www.elsevier.com/locate/jallcom

Dimer splitting of Er^{3+} in $Cs_3Er_2Br_9$

D. Schaniel[a,*], P. Allenspach[a], A. Furrer[a], K. Krämer[b], H.U. Güdel[b]

[a]*Laboratory for Neutron Scattering, ETH Zürich and PSI, CH-5232 Villigen PSI, Switzerland*
[b]*Department of Chemistry, University of Bern, CH-3000 Bern, Switzerland*

Abstract

Inelastic neutron scattering (INS) measurements were performed on the rare earth dimer compound $Cs_3Er_2Br_9$. The crystalline electric field (CEF) parameters were determined. The lack of any exchange splitting associated with the CEF transitions can be explained by the large single ion anisotropy for Er. An energy level scheme is proposed, which was tested with extensive magnetization and specific heat measurements as a function of temperature and magnetic field.

Keywords: Dimers; Rare earth compounds; Crystal fields; Heat capacity; Neutron scattering

1. Introduction

Magnetic clusters are of general scientific interest in order to understand the mechanism of exchange interaction between magnetic ions. $Cs_3Er_2Br_9$ belongs to a whole series of compounds $Cs_3R_2X_9$ (R: rare earth; X: Cl, Br, I) which structurally form rare earth dimers. These materials are of potential use in upconversion lasers, hence an exact knowledge of the energy level scheme is desired [1]. Dimer splittings of up to some 100 μeV due to the exchange interaction have been observed for different rare earths in this structure [2–5]. In the Er^{3+} compound on the other hand no such splitting was observed.

2. Crystal-field splitting

$Cs_3Er_2Br_9$ crystallizes in the space group *R*-3*c*. The point group of the Er^{3+} ion and of the dimer complex $[Er_2Br_9]^{3-}$ are C_3 and D_3, respectively. The 16-fold degenerate ground state multiplet $^4I_{15/2}$ is split into eight Kramers doublets due to the crystalline electric field (CEF). A powdered sample of $Cs_3Er_2Br_9$, sealed under He-atmosphere into an aluminium can, was investigated by neutron spectroscopy on the triple-axis instrument DrüchaL at the neutron spallation source SINQ at PSI Villigen, Switzerland. By performing energy scans at different moduli of the scattering vector $\boldsymbol{Q}$, four inelastic transitions from the ground state doublet to the first excited Kramers doublets were identified as CEF transitions (see Fig. 1). The spectra were analyzed on the basis of the CEF-Hamiltonian

$$\hat{H}_{\mathrm{CEF}} = \sum_{k,q} B_{kq} \hat{U}_{kq} \tag{1}$$

where B_{kq} are the CEF parameters and $\hat{U}_{kq}$ are spherical tensor operators (see, e.g. Ref. [6]). The CEF parameters were determined from the four observed energy transfers and the three corresponding relative intensities as listed in Tables 1 and 2. In Table 1 parameters determined from optical measurements on $Cs_3Lu_2Br_9$ doped with 1% Er [7] are given for comparison.

3. Exchange splitting

From specific heat measurements in zero field we know that there must be a splitting of the Kramers doublets due to exchange interaction [8]. Nevertheless such a splitting could not be found in INS experiments. By adding an exchange term

$$\hat{H}_{\mathrm{ex}} = -2J\hat{\boldsymbol{J}}_1 \cdot \hat{\boldsymbol{J}}_2 \tag{2}$$

to the CEF Hamiltonian defined in Eq. (1) we can calculate the energy splitting of the dimer levels, depending on the value of the exchange constant *J*. *J* was determined by fitting the total Hamiltonian

$$\hat{H} = \hat{H}_{\mathrm{CEF}} + \hat{H}_{\mathrm{ex}} \tag{3}$$

*Corresponding author. Tel.: +41-563-104-192; fax: +41-563-102-939.

E-mail address: dominik.schaniel@psi.ch (D. Schaniel).

0925-8388/01/$ – see front matter
PII: S0925-8388(01)01044-1

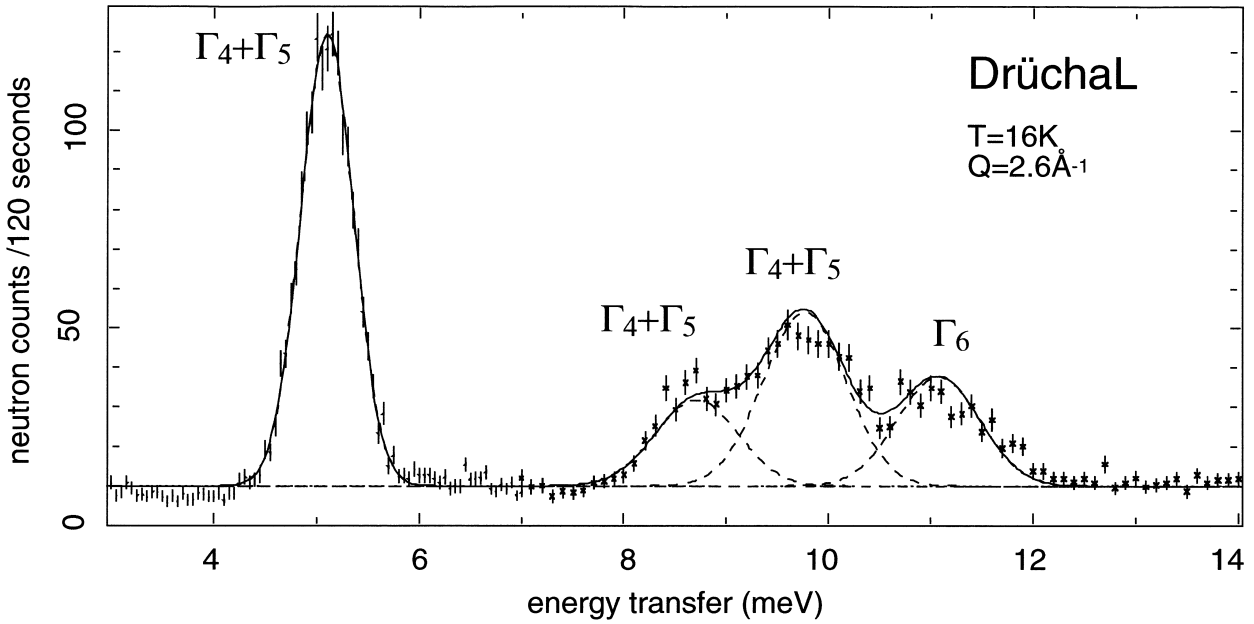

Fig. 1. Observed crystal field transitions in $Cs_3Er_2Br_9$.

Table 1
Fitted CEF parameters for $Cs_3Er_2Br_9$ and parameters from Ref. [7] in meV

	This work	From Ref. [7]
B_{20}	−12.8±1.0	−16.2
B_{40}	−11.7±0.4	−13.2
B_{43}	−301±15	−401
B_{60}	0.95±0.08	1.26
B_{63}	−28.7±2.0	−21.6
B_{66}	10.8±2.0	12.2

to the specific heat in zero magnetic field, yielding $|J| = 0.0011$ meV. Due to the extreme single-ion anisotropy of the Er^{3+} (in excess of 10^2 for $\chi_c/\chi_{a,b}$) the four-fold degenerate dimer ground state splits into two doublets (see Fig. 2) instead of a singlet–triplet separation as found for other rare earths [3,4,9].

In order to check the reliability of our calculation, we compared it with results from the $Cs_3Dy_2Br_9$ compound. There a singlet–triplet splitting of the energy levels was found [9]. In the point-charge model one can extrapolate the set of parameters B_{kq} from one compound to another if the only difference is the rare earth ion. Neglecting small structural changes, the parameters differ only in one factor which is the radial part of the wavefunction of the 4*f*-electrons depending on the number of 4*f*-electrons [10]. This extrapolation led to the parameters given in Table 3. These different sets of parameters result in a very similar CEF-splitting (changing the signs of the B_{43} and B_{63} parameters simultaneously does not change the energy splitting due to the symmetry of the system). The calculation of the exchange splitting was done in the same manner as for $Cs_3Er_2Br_9$, taking $J = -0.003$ meV from Ref. [9]. This led to the expected singlet–triplet splitting. The two geometrically equivalent dimer systems with Er and Dy

Table 2
Observed and fitted energy positions [meV] of CEF transitions and intensities relative to the transition into the first excited doublet in $Cs_3Er_2Br_9$

	E_{obs}	E_{calc}	I^{rel}_{obs}	I^{rel}_{calc}
Γ_6	0	0	–	–
Γ_4,Γ_5	5.1±0.1	5.05	1.00	1.00
Γ_4,Γ_5	8.7±0.2	8.92	0.15±0.03	0.09
Γ_4,Γ_5	9.8±0.2	10.00	0.26±0.02	0.24
Γ_6	11.1±0.2	10.89	0.14±0.01	0.15
Γ_4,Γ_5	–	27.52	–	0.06
Γ_4,Γ_5	–	29.54	–	0.05
Γ_6	–	30.15	–	0.01

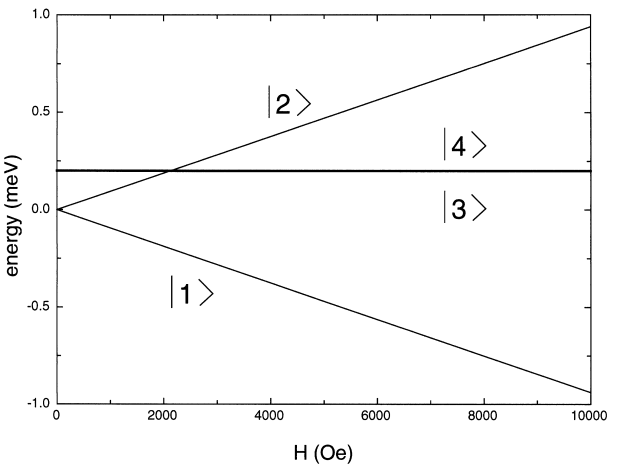

Fig. 2. Proposed dimer splitting as a function of applied magnetic field (parallel to the crystallographic *c*-axis).

Table 3
Extrapolated and experimentally determined [9] parameters for $Cs_3Dy_2Br_9$ in meV

	Extrapolated	From Ref. [9]
B_{20}	−13.9	13.3
B_{40}	−13.6	−12.6
B_{43}	−350	355
B_{60}	1.15	1.49
B_{63}	−34.9	18.5
B_{66}	13.1	14.4

Table 4
Dimer splitting in $Cs_3Er_2Br_9$ and $Cs_3Dy_2Br_9$ calculated as explained in the text

$\|i\rangle$ [meV]	$Cs_3Er_2Br_9$	$Cs_3Dy_2Br_9$
$\|1\rangle$	0	0
$\|2\rangle$	$\leq 10^{-5}$	0.12374
$\|3\rangle$	0.20305	0.12374
$\|4\rangle$	0.20305	0.16450
J [meV]	0.0011	−0.003

result in two completely different exchange splittings. Results of this extrapolation are shown in Table 4. The small splitting of the triplet into a doublet and a singlet is due to the disturbance of the system by the CEF.

4. Magnetization measurements

The magnetization measurements were performed on a Quantum Design PPMS System (extraction method), using different single crystals of $Cs_3Er_2Br_9$. The temperature and magnetic field dependence was studied systematically. Fig. 3 shows some of the temperature scans in different external magnetic fields. The lines are calculations based on the determined CEF parameters and the assumed exchange coupling, using the well-known thermodynamic formula

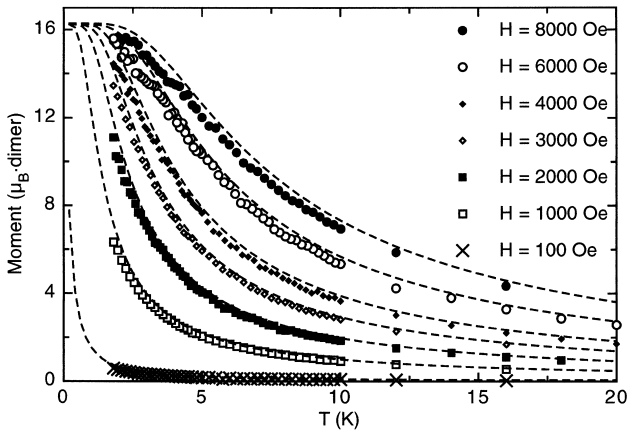

Fig. 3. Magnetization of $Cs_3Er_2Br_9$ in different magnetic fields. The magnetic field is applied parallel to the crystallographic c-axis.

$$M^{\alpha} = g\mu_B\langle\hat{J}^{\alpha}\rangle \quad (4)$$

where α denotes the cartesian coordinates and $\hat{J}^{\alpha}$ the total angular momentum operator. The qualitative agreement is very good and yields a ferromagnetic exchange coupling (positive sign of J) in contrast to other rare earths where we have antiferromagnetic exchange coupling [3,4,9].

5. Specific heat measurements

Further macroscopic investigations were performed to strengthen our arguments about the exchange splitting. Results of specific heat measurements with an external applied magnetic field are shown in Fig. 4. Calculations were done as explained in Ref. [8] on the basis of the assumed energy level scheme and using the β-value for the lattice contribution which resulted from the fit to the zero field data: $\beta = 2.11 \cdot 10^{-2}$ J mol^{-1} K^{-4}. The agreement between data and calculation is satisfying, supporting our view of the energy level scheme. The difference between observed and calculated data in $Cs_3Er_2Br_9$ at the lowest temperatures in the zero-field measurement is due to the onset of magnetic ordering, which takes place at about 1 K.

For comparison with $Cs_3Dy_2Br_9$ we performed similar measurements on this compound. Calculations were done in the same manner as before on the basis of the CEF and the exchange splitting, yielding a good description of the data (see Fig. 5).

6. Conclusions

INS experiments were used to determine the CEF parameters of $Cs_3Er_2Br_9$. The determined parameters give a good description of the observed CEF transitions. The dimer splitting (as shown in Fig. 2) due to the exchange interaction can not be observed since the matrix element for this transition in the neutron scattering cross section vanishes. The proposed dimer splitting leads to a good agreement between calculated and measured thermodynamic properties such as magnetization and specific heat under different external conditions (magnetic field, temperature). We conclude that in the Er compound we have a ferromagnetic exchange coupling which leads together with the high single-ion anisotropy of the Er^{3+} ion to a quite unique configuration compared to other rare earths in similar compounds.

Acknowledgements

Financial support by the Swiss National Science Foundation is gratefully acknowledged.

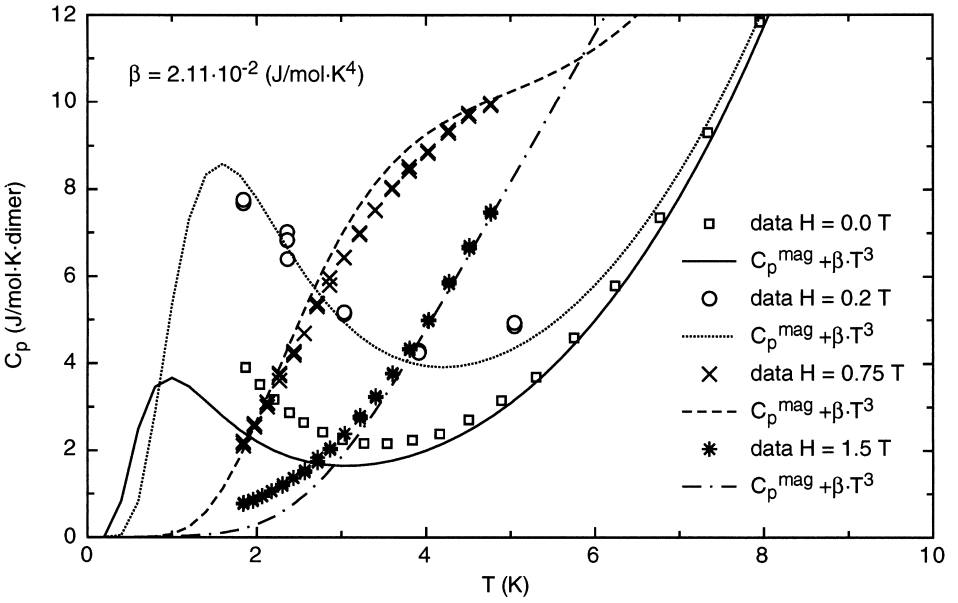

Fig. 4. Specific heat of $Cs_3Er_2Br_9$ in different magnetic fields. The magnetic field is applied parallel to the crystallographic *c*-axis.

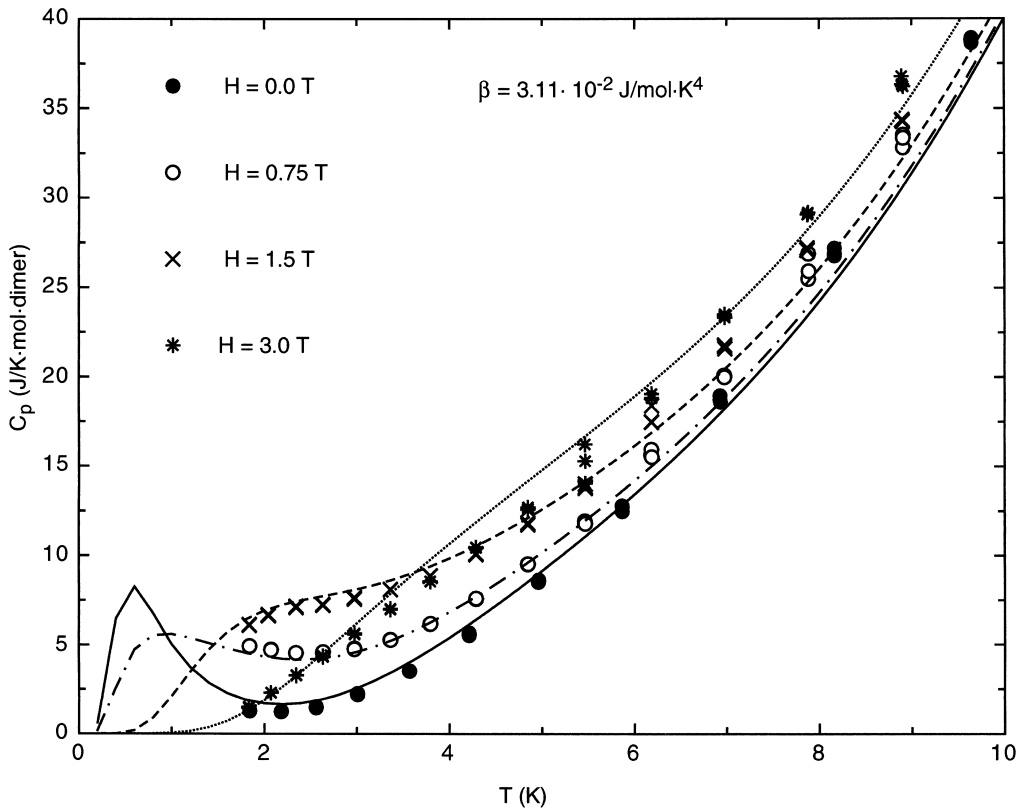

Fig. 5. Specific heat of $Cs_3Dy_2Br_9$ in different magnetic fields (angle between direction of magnetic field and crystallographic *c*-axis was 65°).

References

[1] M.P. Hehlen et al., Phys. Rev. B 49 (1994) 12475.
[2] A. Dönni et al., J. Phys. 49 (1988) C8–1513.
[3] A. Furrer et al., Phys. Rev. Lett. 62 (1989) 210.
[4] A. Furrer et al., Phys. Rev. Lett. 64 (1990) 68.
[5] H.U. Güdel et al., Inorg. Chem. 29 (1990) 4081.
[6] B.G. Wybourne, Spectroscopic Properties of Rare Earths, John Wiley and Sons, 1965.
[7] M.P. Hehlen et al., J. Chem. Phys. 101 (1994) 10303.
[8] D. Schaniel et al., Physica B 276–278 (2000) 1179.
[9] M.A. Aebersold et al., Inorg. Chem. 33 (1994) 1133.
[10] C.A. Morrison, Angular Momentum Theory Applied to Interactions in Solids, Springer Verlag, 1988.